Network-Performance Evaluation for Millimeter-Wave Information-Centric Wireless-Sensor-Network Ecosystem in Actual City

Shintaro Mori
Department of Electronics Engineering and Computer Science
Fukuoka University
8-19-1 Nanakuma, Jonan-ku, Fukuoka 814-0180, Japan
E-mail: smori@fukuoka-u.ac.jp

***Abstract*—This paper presents an evaluation of our research team previously proposed information-centric wireless-sensor-network-based ecosystem for smart-city applications, called mmICWSN. This ecosystem uses millimeter-wave communications for future broadband wireless networks. To demonstrate mmICWSN's feasibility in an actual city, the network performance of our ecosystem was evaluated, including throughput in the application and network layers. The experiment was conducted in Nogata City (Fukuoka, Japan), connecting two 1-km-distant locations. The results indicate that our ecosystem can be verified to communicate with a point-to-point environment.**

Keywords-information-centric wireless sensor network; millimeter-wave communications; smart-city ecosystem.

I. INTRODUCTION

A Wireless Sensor Network (WSN) is an essential foundational technology supporting smart-city application services, where Sensor Nodes (SNs) are heterogeneously interconnected to collect and distribute sensing data, such as real-time streaming and high-capacity data. The data include various demands and priorities, and their transmission method is designed on the basis of several protocols, all of which should be accommodated in the same ecosystem [1]. Millimeter-wave (mmWave) communications [2] and Information-Centric Networking (ICN) technology [3][4] have been gaining attention. MmWave communications have been recognized as a global frontier in future mobile technologies, enabling multi-gigabit data transfer over vast spectrums. ICN is an ideal candidate for a future network architecture that shifts the focus from host locations to data. Namely, the data are named instead of an address, enabling end-users to discover and obtain the data via names, resulting in network abstraction. The named data are handled separately by individual content units, i.e., they can be self-certified and encrypted by their producer, contributing to improved security, in-network caching schemes are also available, i.e., the data are copied and stored in cache memories on network nodes to facilitate further data retrieval.

By applying both mmWaves and ICN to WSNs, our research team previously developed and preliminary evaluated a mmWave Information-Centric WSN-based ecosystem, called mmICWSN that positively affects network performance by improving data delivery [5][6][7]. In one of these papers [7], toward a new sustainable smart-city platform, our mmICWSN can provide a high data rate and low latency with stable connectivity. In addition, we revealed that the ecosystem was ready for deployment in an actual city with prototype implementations. In this paper, an evaluation based on network performance was experimentally conducted to demonstrate the mmICWSN's feasibility in an actual city.

The remainder of this paper is organized as follows. Section II discusses related work. Section III provides a brief overview of the development of mmICWSN. Section IV presents the evaluation results and discussion. Finally, Section V concludes this paper with a summary and mention of future work.

II. RELATED WORK

Zhang et al. [8] identified the open challenges for transport- and network-layer protocols on the basis of a comprehensive simulation study, including congestion control, handover, connectivity, and packet-size control. Khorov et al. [9] investigated emerging wireless systems to provide high-speed data transmissions in mmWave and Terahertz. Note that the transport- and network-layer protocols are unsuitable for these frequency-band communications because of their specific features compared with commonly-used bands due to high signal attenuation and blockage. Kumar et al. [10] experimentally found throughput degradations (collapses) in the 60-GHz band (one of the key frequency bands for mmWaves), and Poorzare et al. [11] analyzed network performances related to this phenomenon under an urban deployment scenario. Yang et al. [12] investigated several congestion-control algorithms, and Vu et al. [13] proposed a state-of-the-art multi-path network protocol for vehicular networks. Netalkar et al. [14] proposed a cross-layer-design end-to-end protocol for fast data delivery in urban micro-cellular networks.

III. ECOSYSTEM DEVELOPMENT

Cellular and satellite telecommunications are the de-facto wireless communication systems for a smart-city ecosystem; however, they are costly to deploy. Although low-power wide-area networks are the primary solutions, they can only transmit a few small data packets within 100-Hz bandwidth below the 1-GHz band. Short-range personal area networks based on IEEE 802.15 standards are used for WSNs. They can conserve power and integrate a high-speed and energy-efficient protocol, but they can be used as a network inside a small regional area. Another global communication system,

 ISBN: 978-1-68558-277-7

wireless local area networks based on IEEE 802.11 standards, known as Wi-Fi, can provide extensive and various connectivity for computers, tablets, smartphones, and Internet-of-Things devices. Similar to the idea of network-system selections [15], Wi-Fi-based networks are the optimal candidate for this purpose, because they have several advantages: low-cost wireless modules are readily available, they can be based on IP networks, and the multiple radio-frequency bands can include unlicensed bands, such as 920 MHz and 2.4, 5, 6, and 60 GHz, without regulations. Our mmICWSN uses the IEEE 802.11 ad/ay-compliant Terragraph (TG) communication system in mmWaves [16].

In our prototype mmICWSN [5][6], we used Cefore [17] for the middleware of the ICN platform. Note that Cefore is an open-source CCNx-based ICN platform available on Linux (Ubuntu). The prototype mmICWSN was implemented not limited to a specific application service but designed on the basis of a reliable and zero-touch design [7]. It was designed to be waterproof since it would be placed in outdoor environments.

IV. EVALUATIONS AND DEMONSTRATIONS

Millimeter waves have been used as an alternative to backhaul, both short-range and high-capacity indoor communications, or radar. Compared with the radio-frequency bands that are currently widely used, the extra attenuations for the link budget of mmWaves, such as rain, oxygen, and hydrophilic materials (e.g., trees, leaves, and humans) must be considered. Note that radio waves in the 60-GHz band are particularly affected by the rain and oxygen. Related studies include the applicability of mmWaves for outdoor applications to provide several hundred meters of coverage. To develop ecosystems in actual cities, it is necessary to conduct additional evaluations. To the best of our knowledge, there have been few experiments regarding mmWave long-distance data transmissions; hence, we believe that the contribution of this paper is valuable.

The node devices described in Section III were deployed at a community center and school in Nogata City (Fukuoka, Japan), as shown in Figure 1. The community center and school are three-story buildings, and the node devices were placed on their rooftops. In accordance with the three-dimensional map provided by the National Geographical Institute [18], their altitudes are respectively 7.5 and 16 m, and the straight-line distance between them is 1 km. Across the wireless link, there are a river, road, bridge, and car park, as shown in Figure 2, which might affect radio propagation. The river is the Onga River and the riverside area is well maintained and covered with grass and aquatic plants. During the experiment, the river surface was flat and calm, with no significant waves, i.e., factors affecting mmWave propagation were not observed. The Kanroku Bridge crosses the river and is connected to the main national road. Nogata City is an inter and suburban city between large cities (e.g., Fukuoka City and Kitakyushu City), but the amount of traffic is not dense. The riverside area in front of the community center is used as a car park, and several dozen cars were parked there.

Figure 3 shows the field view of the experimental site. Figures 3(a) and (b) and Figures 3(c) and (d) show the field

Figure 1. Location map of transmitter- and receiver-side nodes

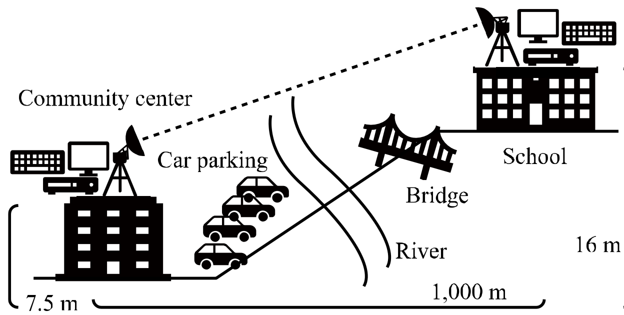

Figure 2. Outline of experimental environment

TABLE I. SPECIFICATION OF TG DEVICE

Terms	***Values***
Radio frequency	58.32 GHz (57–66 GHz) with 2.16 GHz
Transmission power	56 dBm (EIRP)
Antenna	Phased array antenna with dish Gain: 40 dBi Scan range: ±3°, Beam width: ±1°
Dimensions	355 × 355 × 315 mm
Weight	3 kg

views of the rooftops of the community center and school, respectively. As shown in Figures 3(a) to (d), the mmICWSN node devices were connected to the BeMap MLTG-CN/LR [19] as the mmWave TG device, and the specifications of this device are listed in Table I. In the experiment, two MLTG-CN/LR devices communicated with each other, and the available communication distance was up to 1 km, according to the catalog specifications. Throughout the experiment, the Modulation and Coding Scheme (MCS) index was automatically set as 9. Table II shows the parameter settings regarding adaptive rate control in the IEEE 802.11 ay. Note that IEEE 802.11-compliant Wi-Fi systems achieve effective (high-throughput) data transmission to the control modulation scheme, code rate of error-correcting code, and repetition code based on wireless channel condition, and their combination is pre-defined as MCS settings. Figure 3(e) shows a photo taken behind the dish antenna on the school rooftop toward the community center. The community center is located at the red marking, where the opposite node was

TABLE II. MCS SETTINGS IN SINGLE CARRIER PHYSICAL MODE

Index	*Modulation method*	*Code rate*	*Repetition*	*Data rate* (Mbit/s)
1	BPSK	1/2	2	385
2	BPSK	1/2	1	770
3	BPSK	5/8	1	963
4	BPSK	3/4	1	1,155
5	BPSK	13/16	1	1,251
6	QPSK	1/2	1	1,540
7	QPSK	5/8	1	1,925
8	QPSK	3/4	1	2,310
9	QPSK	13/16	1	2,503
10	16-QAM	1/2	1	3,080
11	16-QAM	5/8	1	3,850
12	16-QAM	3/4	1	4,620

TABLE III. PHYSICAL-LAYER INFORMATION IN EXPERIMENT

Terms	*Antennas are matched*	*Antennas are mis-matched*
Radio channel	Ch 2 (60.48 GHz with 2.16 GHz)	
RSSI	-64 dBm	-62–63 dBm
MCS settings	8–9	6–9
Beam index	30 / 30	30 / 5

placed. As shown in Figure 3(e), the line of sight between the transmitter- and receiver-side nodes can be clearly maintained. The weather was cloudy during the experiment, i.e., the possibility of rainfall attenuation to degrade the mmWaves-band radio propagation could be ignored.

The experiment was conducted for two different scenarios: one in which both elevation and azimuth angles were appropriately adjusted (the antennas were matched), and the other when they were slightly offset (the antennas were mismatched). The status information of the physical layer for these scenarios is summarized in Table III. Note that, in the MLTG-CN/LR device, the antenna's front space is divided into a grid pattern in terms of elevation- and azimuth- angles, then each sub-region is assigned a beamforming index. The most central beam direction on the antenna surface is when the beamforming index is 30. Figure 4 shows the experimental results, which both (a) and (b), (c) and (d), and (e) and (f) are Transmission Control Protocol (TCP) with the CUBIC algorithm, User Datagram Protocol (UDP), and ICN performance, respectively. In Figures 4(a) to (d), iPerf3 [20], which is a well-known network-performance measurement tool, was used to measure TCP/UDP performance at every 1 s interval for 90 s. Note that the nodes in the community center and school were assigned as server and client nodes in the iPerf3 settings. Figures 4(e) and (f) show the results of retrieving the different data using Cefore [17].

As shown in Figure 4(a), the average TCP throughput was 941 and 94.4 Mbit/s for when the antennas were matched and mismatched, respectively. The TG antenna is a parabolic dish type; thus, even a few degrees of angle misalignment can cause significant TCP throughput degradation. For TCP congestion control, as shown in Figure 4(b), the average congestion-window size was 1.26 and 0.967 Mbytes; hence, there was a 39.3% difference. In the curve when the antennas

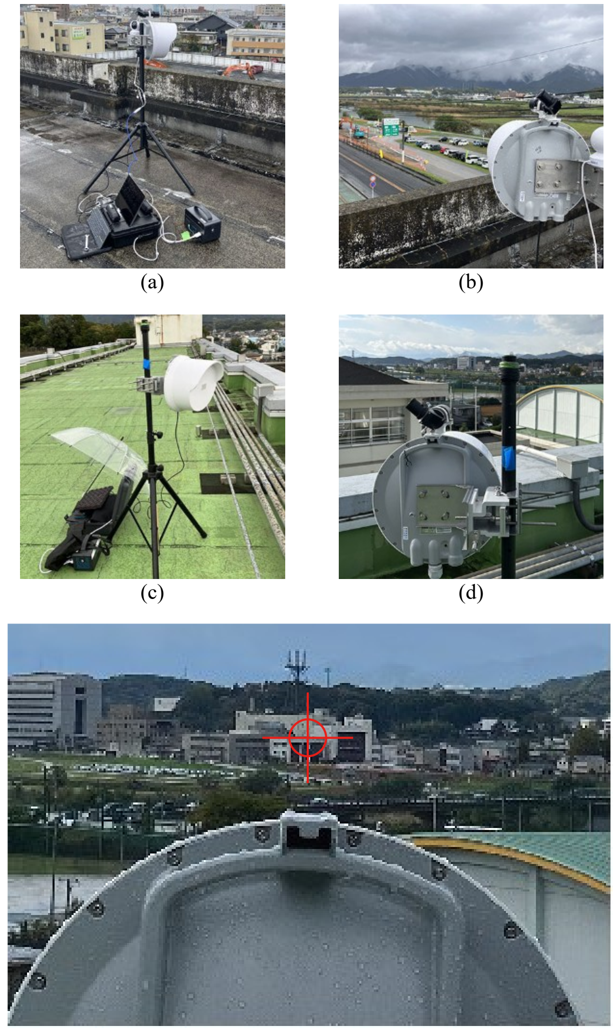

(a) (b) (c) (d) (e)

Figure 3. Field view of transmitter- and receiver-side nodes on rooftop of community center and school buildings

were matched, several attempts were made to increase the congestion-window size.

As shown in Figure 4(c), the average UDP throughput was 902 and 93.3 Mbit/s for the two scenarios, respectively. In the curve when the antennas were matched, there were regions where UDP throughput temporarily decreased. The reason for this decrease is that automatic retransmission requests and forwarding-error-control mechanisms are omitted, resulting in these dramatic degradations. The results in Figure 4(a) indicate no degradation because the congestion-control mechanism in TCP is available and useful works. Figure 4(d) shows the packet-error probability for UDP transfer; the averages were 0.0294 and 0.903 for the matched and mismatched scenarios, respectively. When the antennas were mismatched, many packet losses occurred, which affected not only UDP throughput but also that of TCP, as shown in Figures 4(a) and (c).

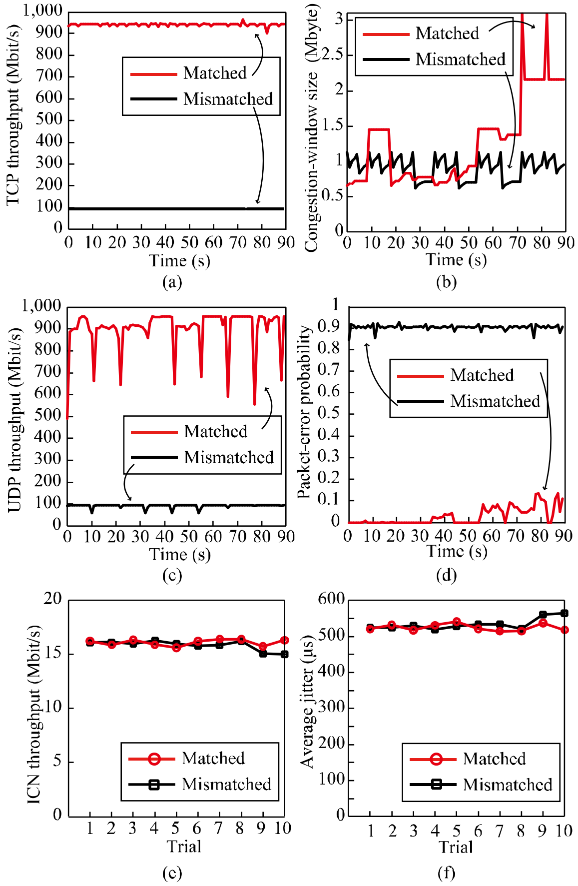

Figure 4. Experimental results

As shown in Figure 4(e), the average ICN throughput was 16.1 and 15.8 Mbit/s for the two scenarios, respectively. The ICN throughput was significantly smaller than that of TCP or UDP because Cefore has a bottleneck. In mmICWSN, the ICN layer was stacked on the TCP/UDP layers. Thus, due to the middleware implementation in Cefore, if the maximum data-transmission bandwidth is set as the maximum value, the failure probability of data registration, storage, and transfer becomes worse. As shown in Figure 4(f), the average jitter was 525 and 534 μs for the two scenarios, respectively. ICN throughput and jitter did not significantly differ between the two scenarios. In accordance with these results, we found that the performance of TCP/UDP/IP protocol stacks was not affected by that of the ICN-layer protocol. We also experimentally verified that we could obtain sufficient network performance for mmICWSN in an actual city.

V. Conclusion and Future Work

Our research team evaluated the feasibility of the network performance in the TCP, UDP, and ICN protocols with mmICWSN. From the experimental results, we found that it was necessary to improve the ICN throughput by modifying the Cefore settings, and the antenna placement for mmWaves was sensitive to a few degrees of angle. Through the demonstration of the mmWaves experiment, the developed system could be applicable to long-distance wireless transmission in an actual city. For future work, we plan to deploy mmICWSN for practical smart-city applications, such as smart agriculture. In detail, we will develop a new ecosystem that supports an on-demand and real-time video and image forwarding platform for a common demand for smart-agriculture applications.

Acknowledgments

This work was partly supported by JSPS KAKENHI Grant Number JP25K15104 and NICT Japan, Grant Number JPJ012368C05601. We are grateful to Dr. Kenji Kanai for their helpful discussions, and to Nogata City and Advantech Japan for their help with the experiments.

References

[1] P. Mishra and G. Singh, “6G-IoT framework for sustainable smart city: Vision and challenges,” *IEEE Consumer Electronics Mag.*, pp. 1–8, Sept. 2023.

[2] K. Aldubaikhy, W. Wu, N. Zhang, N. Cheng, and X. Shen, “MmWave IEEE 802.11ay for 5G fixed wireless access,” *IEEE Wireless Communications*, vol. 27, no. 2, pp. 88–95, Apr. 2020.

[3] B. Ahlgren, C. Dannewitz, C. Imbrenda, D. Kutscher, and B. Ohlman, “A survey of information-centric networking,” *IEEE Communications Mag.*, vol. 50, no. 7, pp. 26–36, July 2012.

[4] L. C. M. Hurali and A. P. Patil, “Application areas of information-centric networking: State-of-the-art and challenges,” *IEEE Access*, vol. 10, pp. 122431–122446, Nov. 2022.

[5] S. Mori, “Zero-touch-design information-centric wireless sensor networking with availability assurance,” *International J. Advances in Networks and Services*, vol. 16, no. 3&4, pp. 63–74, Dec. 2023.

[6] S. Mori, “Test-field development for ICWSNs and preliminary evaluation for mmWave-band wireless communications,” *Proc. IEEE CCNC 2024*, Las Vegas, USA, Jan. 2024, pp. 1–2, doi: 10.1109/CCNC 51664.2024.10454799.

[7] S. Mori, “Development of UAV-aided information-centric wireless sensor network platform in mmWaves for smart-city deployment,” *International J. Advances in Networks and Services*, vol. 17, no. 3&4, pp. 105–115, Dec. 2024.

[8] M. Zhang, et al., “Will TCP work in mmWave 5G cellular networks?,” *IEEE Communications Mag.*, vol. 57, no. 1, pp. 65–71, Jan. 2019.

[9] E. Khorov, A. Krasilov, M. Susloparov, and L. Kong, “Boosting TCP & QUIC performance in mmWave, Terahertz, and Lightwave wireless networks: A survey,” *IEEE Communications Surveys & Tutorials*, vol. 25, no. 4, pp. 2862–2891, Aug. 2023.

[10] R. Kumar, et al., “TCP BBR for ultra-low latency networking: Challenges, analysis, and solutions,” *Proc. IFIP Networking 2019*, Warsaw, Poland, May 2019, pp. 1–9, doi: 10.23919/IFIPNetworking. 2019.8816856.

[11] R. Poorzare and A. C. Augé, “How sufficient is TCP when deployed in 5G mmWave networks over the urban deployment?,” *IEEE Access*, vol. 9, pp. 36342–36355, Mar. 2021.

[12] W. Yang, et al., “A measurement study of TCP performance over 60GHz mmWave hybrid networks,” *Proc. WoWMoM 2022*, Belfast, UK, June 2022, pp. 300–305, doi: 10.1109/WoWMoM54355.2022.00057.

[13] N. T. T. Vu, H. D. Le, K. D. Dang, C. T. Nguyen, and A. T. Pham, “Performance analysis of multipath TCP over FSO/mmWave vehicular networks,” *Proc. ATC 2023*, Da Nang, Vietnam, Oct. 2023, pp. 172–177, doi: 10.1109/ATC58710.2023.10318939.

[14] P. Netalkar, J. Chen, and D. Raychaudhuri, “mmCPTP: A cross-layer pull based transport protocol for 5G mmWave networks,” *Proc. IEEE/IFIP NOMS 2023*, Miami, USA, May 2023, pp. 1–9, doi: 10.1109/NOMS56928.2023.10154364.

[15] A. U. H. Hashmi, et al., “Effects of IoT communication protocols for precision agriculture in outdoor environments,” *IEEE Access*, vol. 12, pp. 46410–46421, Mar. 2024.
[16] Terragraph, https://terragraph.com/ (retrieved: Jan. 2025).
[17] Cefore, https://cefore.net/ (retrieved: Jan. 2025).
[18] NGI, https://www.gsi.go.jp/ENGLISH/ (retrieved: Jan. 2025).
[19] BeMap, https://www.bemap.co.jp/ (retrieved: Jan. 2025).
[20] iPerf3, https://iperf.fr/ (retrieved: Jan. 2025).

 ISBN: 978-1-68558-277-7